NUCLEAR INSTRUMENTS AND METHODS 79 (1970) 43–50; © NORTH-HOLLAND PUBLISHING CO.

A SCINTILLATION COUNTER ARRAY FOR DETECTION OF HIGH ENERGY NEUTRONS

A. S. L. PARSONS* and P. TRUOEL†

Lawrence Radiation Laboratory, University of California, Berkeley, California 94720, U.S.A.

and

P. A. BERARDO, R. P. HADDOCK, L. VERHEY and M. E. ZELLER+

University of California at Los Angeles, California, U.S.A.

Received 22 September 1969

An array of 32 liquid scintillation counters used to detect neutrons in the energy range 20 to 340 MeV is described. Each unit consisted of a cylinder 45 cm long and 7 cm diameter, with the axis of the cylinder parallel to the incident neutron direction. The array was calibrated in the above energy range by use of neutron-proton elastic scattering. The average efficiency was 0.45. Some secondary properties of the array have been studied and are described.

1. Introduction

In order to measure differential cross sections for the process $\pi^- p \rightarrow n\gamma$ we have constructed and calibrated an array of neutron detectors. The requirements of this experiment dictated the following design and operational criteria for the neutron counters:

1. High detection efficiency for neutrons ranging in energy from 20 to 340 MeV.

2. Good spatial resolution per counter, with a total array size which would match the solid angle of the spark chamber which detected the photon.

3. Well-determined detection efficiency over the necessary neutron energy region.

The construction and calibration of similar detectors has been described by several authors[1-6]); however, the demands of good spatial resolution, high efficiency, and accurate efficiency determination were not so great in their work as in this application.

The method of calibration used was neutron-proton elastic scattering. Detection of the recoil proton tags the presence of a neutron in a well-defined direction, and a counter placed in this "beam" of neutrons may be calibrated. This method of tagging has been previously used by other authors[7]).

2. Design and construction

To make the angular resolution of the neutron compatible with other contributions to the resolution, a 20-mr definition was required. Considerations of the solid angle, time-of-flight path, and matching of array size to the photon spark-chamber solid angle led to the choice of a neutron detector consisting of a 7-cm-diameter cylinder, 45 cm long, placed 365 cm from the target. The detection array contained 32 such cylinders mounted 9 cm apart (center to center), as shown in fig. 1. This spacing was chosen after preliminary measurements on the probabilities of scattering of incident neutrons from one counter into another.

The scintillating material chosen was a liquid, NE 224[8]). The base for the liquid was pseudo-cumene, which has the advantage over other possible solvents that it does not interact significantly with lucite and other materials. Liquid scintillator is superior to most solids, as it has a higher hydrogen content and lower light-absorption coefficient in the spectral region of the scintillations. The major drawback of liquids is their large dependence of volume on temperature. This required installation of vent lines on each counter to permit expansion of the liquid without breaking the container. Air-conditioning the region around the neutron-counter array minimized the effects of temperature fluctuations during the experiments.

The basis for the construction was a lucite tube of 7.6 cm outside diameter with a 0.32-cm wall. Details are shown in fig. 2. Before the design was completed, tests were made on prototype counters. The type of reflective surface placed around the tube was studied as a function of "absorption length" along the tube for scintillations from a ^{60}Co source. A spectral reflecting surface was chosen. The stability of the response of the liquid scintillator when it is in contact with various components of the counter, i.e. lucite, lucite

* Now at Rutherford High Energy Laboratory, Berkshire, England.

† On leave from Schweizerisches Institut für Nuklearforschung, Zürich.

+ Present address: Department of Physics, Yale University, New Haven, Conn.

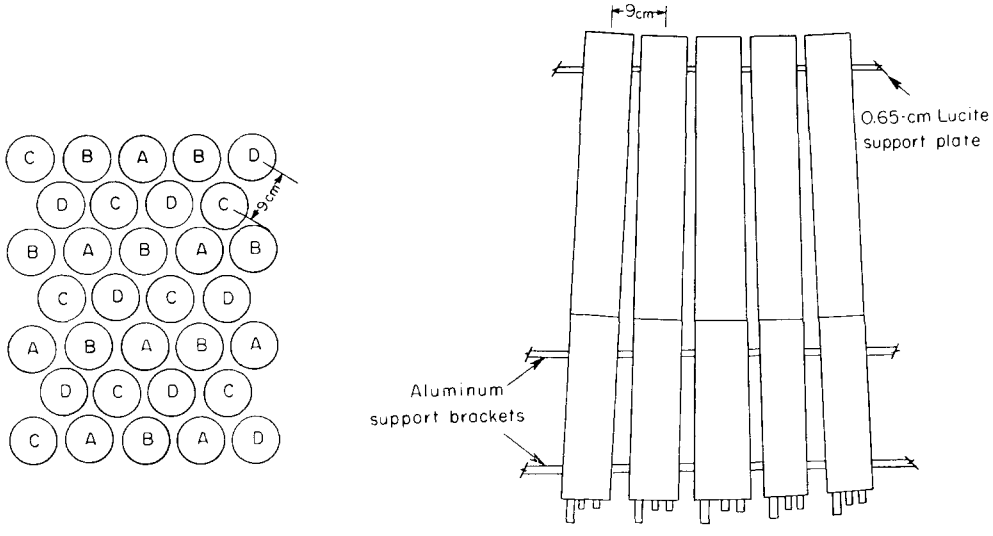

Fig. 1. The neutron counter array. (a) Neutron view; the letters assign counters to one of four independent time-of-flight measuring systems. [For much of the data taking A, B and C, D were combined to form two systems only.] (b) Plan view; the counters focus on a target at 366 cm from the front face.

cement, air, etc., was also studied. For the materials used in the counters, no significant loss in response was observed during several months of testing.

The photomultiplier tube used was an RCA 8575. This tube was chosen because of its high quantum efficiency (approximately 28%), high gain (approximately 10^8), and low dark current (approximately 10^{-9} A).

An important factor in the design of the system was the type of discriminator to be used with the phototube. We chose an EGG type 140 discriminator[9]) which has the following property: the presence of an output pulse is determined when the leading edge of the pulse exceeds a given pulse height (as in a conventional discriminator); the timing of the output pulse is determined when the input pulse, appropriately clipped, crosses zero. The single unit has the properties of a system that would normally require two discriminators and an "AND" circuit. The EGG 140 is "fixed level" and the bias on a given counter was adjusted by varying the high voltage on the phototube. The dynode signals were used to give pulse-height information.

The biases on the 32 counters were set to be equal in the following manner. With a ^{60}Co source placed at a standard geometrical position on a counter, two pulse-height distributions were obtained: one gated by the anode discriminator, and one ungated. The high voltage on the tube was then adjusted until the lower limit of the gated spectrum corresponded to the upper limit of the ungated ^{60}Co distribution (see fig. 3). The lower limit is determined by the discrimination level on the

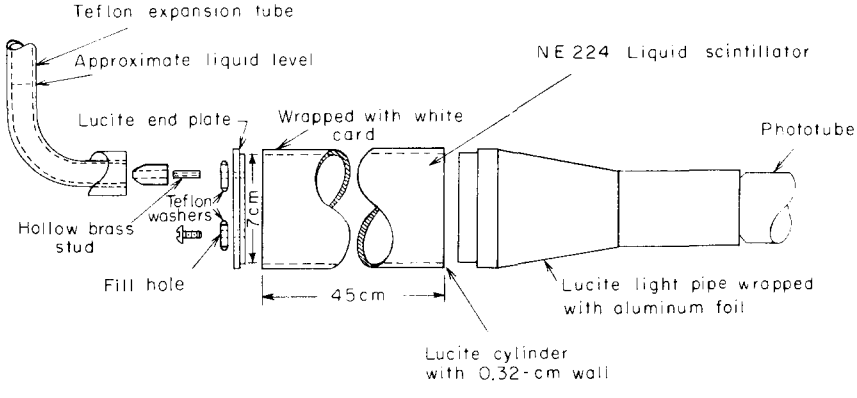

Fig. 2. Details of the construction of one neutron counter.

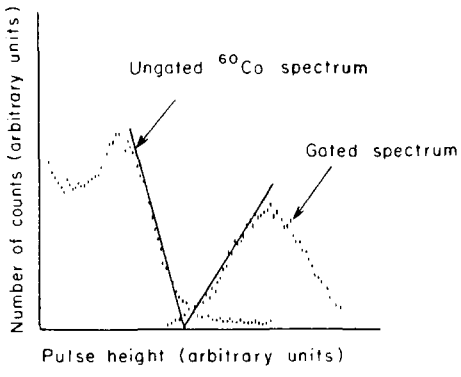

Fig. 3. Pulse-height spectra used in setting phototube bias.

anode signal; the upper limit represents the Compton scattering end point of ^{60}Co. Each tube is thereby set at an electron bias level of about 1.3 MeV. The reproducibility of this method in terms of the efficiency of the counters for neutron detection was checked extensively at 112 MeV neutron kinetic energy and to a lesser extent at 50 and 20 MeV. Comparison of the efficiencies of eight counters as well as the efficiency of one counter on several different occasions is shown in fig. 4. This method allowed the bias, in terms of the threshold for a given energy deposited in the scintillator, to be set at the same level for each counter regardless of the gain of the phototube or the discriminator threshold.

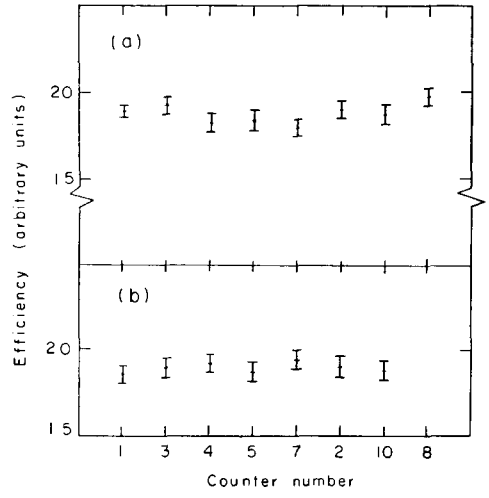

Fig. 4. Comparison of the efficiency at 112 MeV, (a) for several counters, (b) for one counter on different occasions.

3. Calibration

The array was calibrated by use of neutron-proton elastic scattering. The setup is shown in fig. 5.

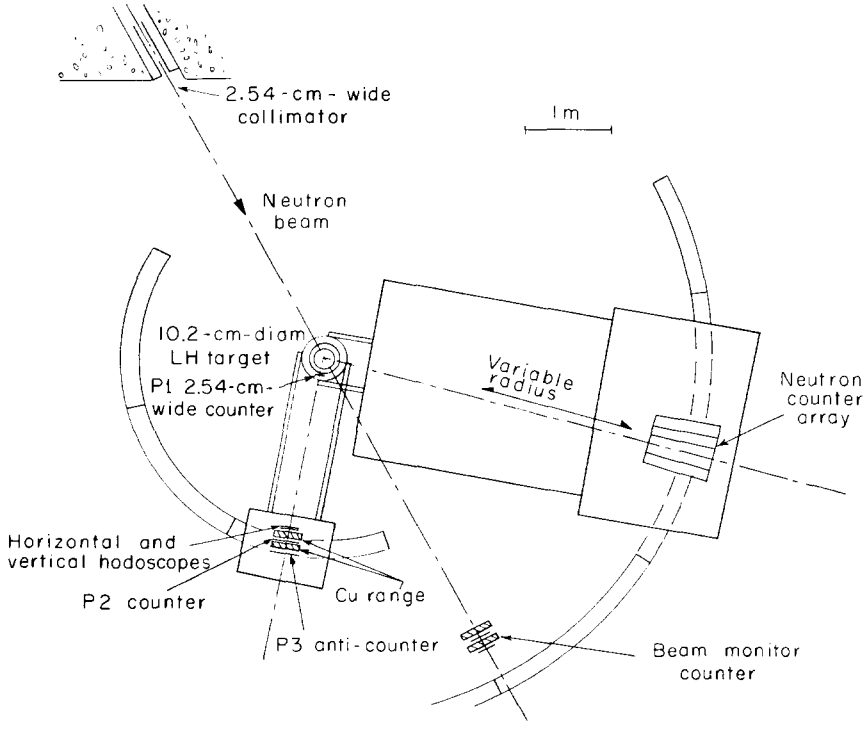

Fig. 5. Neutron proton elastic scattering setup. The neutron counter array is offset to allow it to be placed as close as possible to the π^- beam in the radiative capture experiment.

The neutron beam was obtained from the Berkeley 184-inch cyclotron. Apart from one calibration measurement at 340 MeV neutron kinetic energy, the beam was obtained by stripping 450-MeV deuterons on an internal beryllium target. This yielded a beam of 204-MeV neutrons with full width at half height of 60 MeV. After collimation, the beam at the liquid hydrogen target was 3.2 cm high and 2.5 cm wide. A Polaroid film exposed just downstream from a CH converter in the beam line determined these dimensions. For the 340-MeV measurements the neutrons were produced by 730-MeV protons on beryllium. The spectrum in this case had a peak at 650 MeV, a full width at half height of about 100 MeV, and a long low-energy tail. For this energy, collimation was less effective, and the limits of the beam at the target were consequently less well defined.

The hydrogen target, a 10.15-cm-diameter vertical cylinder 20 cm high, was the same as used in the main experiment. To allow a variable target thickness, the target cylinder was divided by a 0.02-cm-thick vertical mylar wall perpendicular to the beam. For the calibration experiment both halves were filled. The vacuum jacket was made of 0.12-cm aluminum with 0.07-cm mylar entrance and exit windows. The recoil scattered protons were detected in a differential-range telescope. This telescope consisted of a 2.5×2.5-cm counter placed 14.3 cm from the target, counters in front of and behind the range at about 200 cm radius, and an anti-counter behind the differential range. The counter close to the target (P1) and the well-collimated incident neutron beam defined an interaction volume in the target which excluded the flask wall[5]). This definition reduced the background due to events not associated with hydrogen to about 1%.

The direction of the proton in a given event was determined by the counter P1 and an 8×8 array of 1.27-cm crossed hodoscope counters placed in front of the differential range counters at a radius of 196 cm from the target center. The neutron counter array was placed 365 cm from the target, the same radius as for the main experiment. The counter P1 also provided a start signal for measurement of the neutron time of flight.

At 205 MeV incident energy, runs were taken at eight angles corresponding to scattered-neutron energies between 20 and 140 MeV. The upper limit was set by the low energy of the recoil proton. At 650 MeV incident energy the only practical neutron energy was around 340 MeV. This energy yielded a maximum in the event rate, since the range in the proton telescope was not too great, and the solid-angle transformation factors were still favorable. At each angle the amount of copper range in the proton telescope was set to give the largest stopping-proton rate in the differential range. The shape of the range curves obtained reflected the incident neutron spectrum. The differential range was 2.9 g/cm^2 of copper.

A PDP5 computer was used to monitor the apparatus and to provide a buffer for data storage on magnetic tape. Upon an event trigger, normally a stopping proton, the addresses of the hodoscope and neutron counters that fired and the neutron time of flight and pulse height were recorded and monitored for system stability.

At each angle more than 5×10^4 protons were stopped, yielding about 10^4 events in which a neutron also was detected.

Measurements with empty target were also taken; they showed a contribution of 1 to 2% to the event rate with target full. Random neutrons were less than 1% of the events, and were monitored by use of the time-of-flight information.

The calibration experiment was used to measure the efficiency of the array and to check the spatial- and time-resolution function for reconstruction of the two-body kinematics in the radiative-capture experiment. The background-free sample of two-body events from the neutron-proton scattering data was well suited for this check.

4. Efficiency calculation

The measurement of the efficiency was closely coupled to a Monte Carlo simulation of the experiment. This program to generate events included the following effects:

a. A uniform spatial distribution of neutrons in the beam over the area measured.

b. The measured energy distribution of neutrons.

c. Multiple scattering of protons in the target, vacuum jacket, and counters.

d. Energy selection of protons due to the differential range.

e. Interaction of neutrons in the target and vacuum jacket.

f. Computation of the geometrical potential path length (PPL) of the neutron in a neutron counter, expressed as the fraction of active counter a given neutron can traverse if it does not interact.

g. Neutral cross-scattering in the neutron counter array; in this process a neutron enters one counter and scatters into another without the recoil's being detected, but a signal is produced in the second counter.

This effect was measured in a secondary experiment to be described.

Besides the obvious geometrical effects, (c) and (g) were the main contributions to the resolution function.

Since the length of a counter was much larger than its radius, the PPL had a nonnegligible probability of being less than one. The average PPL determined from the Monte Carlo program was used to linearly normalize all efficiencies to a full counter length of 45 cm. The final efficiency is thus the ratio of the experimental to the normalized geometrical efficiency. This efficiency is shown in fig. 6 and table 1 as a function of neutron kinetic energy. The calculated efficiency[10]) for a single counter of the appropriate size is shown in fig. 6. The efficiency of our total array is expectedly higher, since we detect many of the outscattered neutrons elsewhere in the array.

5. Event reconstruction and Monte Carlo check

Since the efficiency is strongly dependent on the Monte Carlo calculation of the mean PPL, it is important to check that the program correctly simulates the data. Such a check is made with an event-by-event fitting program. Both the Monte Carlo-generated events and the data were subjected to the same analysis routine. This routine used the measured quantities for each event, including the beam direction, mean beam momentum, angles of scattered neutron and proton, and neutron time of flight to compute an overall χ^2 for the event to fit the elastic scattering process. The errors used in computing this χ^2 were geometrical only, i.e., neutron and proton scattering were not included. The extent to which events lie anomalously far from a χ^2 of zero therefore reflects the amount of

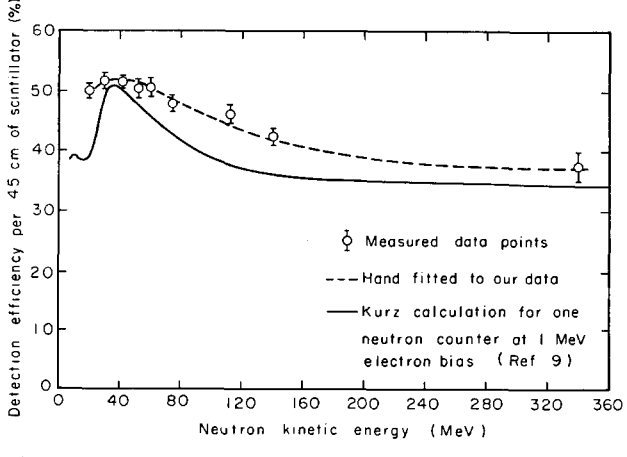

Fig. 6. Detection efficiency of neutron counter array vs neutron kinetic energy.

TABLE 1
Detector efficiency as a function of neutron kinetic energy.

T_1[a] (MeV)	T_n[b] (MeV)	R_n[c] (cm)	θ_n (deg)	θ_p (deg)	Range (g/cm²)	Diff. range (g/cm²)	No. of protons stopped (exp.)	No. of n-p coincidences	Empty target corrections	Random events corrections	No. of protons stopped (M. Carlo)	No. of n-p coincidences	No. of neutron counter lengths traversed	Efficiency per counter length
203	20	365	70.0	18.1	26.0	2.9	49668	9163	0.70%[d]	0.8%	3359	1411	1220.0	50.1±1.2
203	30	365	65.8	22.0	23.4	2.9	49817	11010	0.70%[d]	0.7%	2630	1277	1121.0	51.8±1.2
203	40	365	61.6	26.0	21.1	2.9	95594	21900	0.72%	0.6%	4010	2070	1777.1	51.6±1.1
203	52	365	58.0	29.4	17.18	2.9	11327	2587	0.75%	0.6%	3642	1912	1647.5	50.5±1.4
203	60	365	55.3	32.0	15.8	2.9	140909	32961	0.70%	0.6%	3217	1761	1528.1	50.7±1.1
203	74	365	51.2	36.0	11.4	2.9	99661	22898	0.78%	0.6%	2390	1313	1142.6	48.0±1.2
203	112	365	40.0	45.9	4.43	2.9	82261	17042	0.58%	0.4%	1496	778	668.3	46.3±1.6
203	140	365	31.3	56.0	0.0	0.0	50103	10258	2.10%	0.8%	1931	1091	932.2	42.6±1.2
650	340	365	36.05	45.0	57.9	5.8	2182	405	0.70%[d]	0.6%	660	363	325.7	37.6±2.4
203	30	183	67.4	22.0	23.4	2.9	37192	10150	1.30%	0.5%	1030	778	512.5	55.0±2.6
203	60	183	56.9	32.0	15.8	2.9	282620	75031	1.30%[e]	0.4%	7756	5707	3810.2	54.3±0.9
203	112	183	41.4	45.9	4.43	2.9	314700	76856	1.10%[e]	0.4%	2500	1904	1247.9	49.3±1.5

[a] Incident neutron energy.
[b] Energy of the scattered neutron.
[c] Radius of neutron counter array.
[d] Extrapolated.
[e] Scaled from 365-cm run.

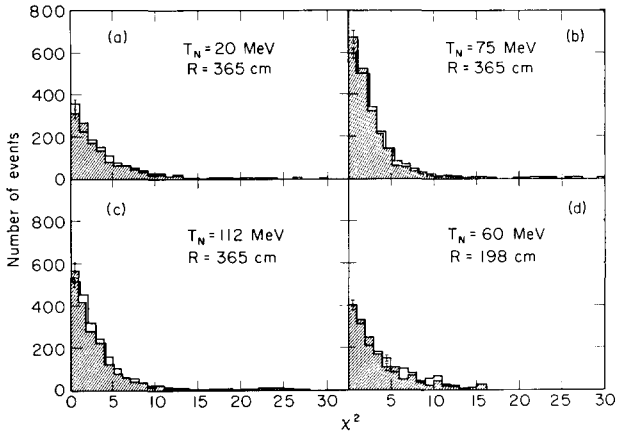

Fig. 7. χ^2 distributions for the n-p elastic scattering data (unshaded) and for the Monte Carlo (shaded) simulation of the process. The Monte Carlo distribution has been normalized to the same number of events as the data.

such scatterings. The comparison of χ^2 distribution for data and the Monte Carlo calculation is shown in fig. 7a–c for three energies.

A second check on the Monte Carlo program was made by analyzing data taken with the array at a 198-cm radius. The geometrical effects of this decreased distance are quite large, but since the Monte Carlo program effectively removes the geometrical dependence from the efficiency per PPL, a comparison of the efficiencies measured at the two radii is a check on the Monte Carlo calculation. Fig. 7d compares the χ^2 distribution for the data and Monte Carlo for 60-MeV neutron energy with the array at 198 cm.

6. Neutral and charged cross scattering

Neutral cross-scattering is defined as the detection of a neutron in a counter other than that which it entered; charged cross-scattering is a similar effect except that the recoil is also detected in the first counter. Both processes have the effect of broadening the spatial resolution function. In practice the charged scattering is less serious, since the counter which the neutron first entered can be found by choosing the counter that gives the best fit to the two-body kinematics hypothesis.

Some properties of the charged cross-scattering are summarized in figs. 8 and 9. Fig. 8 shows the frequency of charged cross-scattering or multiple events vs the kinetic energy of the neutron. Fig. 9 shows the spatial and time difference between two counters participating in a double-counter event for two energies. The sharply peaked time difference distribution indicates that there is only a small contribution to the doubles from random neutrons. The spatial distribution shows that large spatial displacements are not uncommon, and presumably correspond to a neutron's traversing several counters before reconverting. The peak at small distances contains the contributions from the charged recoil particles reaching adjacent counters.

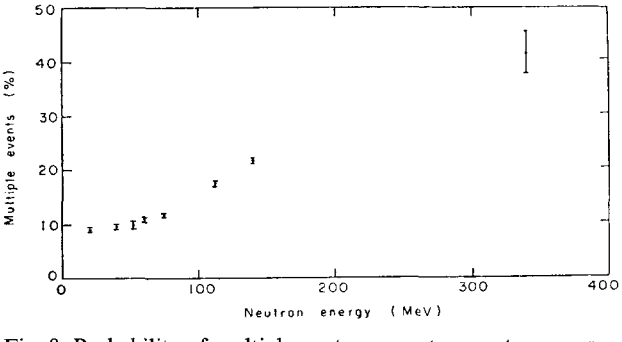

Fig. 8. Probability of multiple neutron counter events vs energy of the neutron.

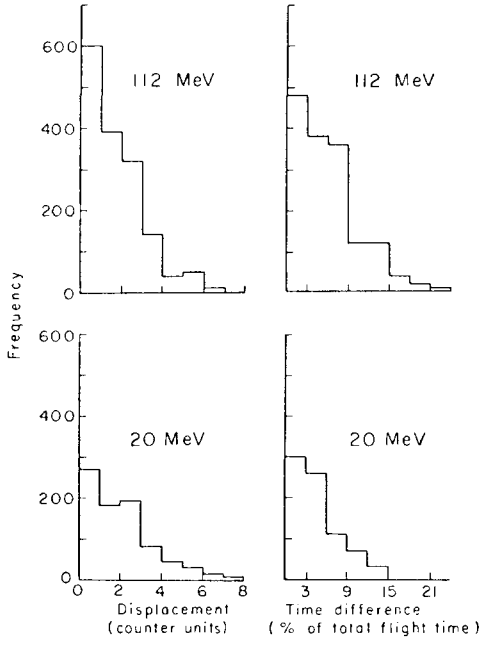

Fig. 9. Relative spatial and time distribution of double neutron counter events. One counter unit is nearest neighbor, two counter units is next nearest neighbor, etc.

To study neutral cross-scattering the neutron counter array was placed at 198 cm from the target, thus increasing the rate at which neutrons entered the central counters. For each energy two runs of about 10^5 events were recorded, one with the complete array, the second with one of the central counters removed. The loss of

events in all the counters due to the removal of one counter, corrected for charged cross-scattering from that counter, was taken as a measure of the neutral cross scattering. Distributions were measured at three energies, and are presented in fig. 10. The assumption is made that these distributions measured at 198 cm radius can be used to describe cross-scattering at 365 cm. It is unlikely that the radius of the array is of primary importance for this process. The probability of neutral cross-scattering vs energy is shown in fig. 11.

7. Application

The efficiency quoted is the efficiency for detection of the neutron anywhere within the array, not necessarily within the counter initially entered. This efficiency can be carried over to the main experiment, as long as a suitable resolution function is used and some correction factors are applied. These corrections, arising from the lack of exact correspondance between the two experimental arrangements, will now be described.

The most significant correction arose from the difference in the distribution of neutrons entering the array. In the radiative-capture experiment the distribution was essentially uniform; in the calibration experiment the selection of events by the proton telescope produced a distribution which was peaked at the center of the array, and fell almost to zero at the perimeter, simulating an infinite array of counters. Since the efficiency is defined for detection of a neutron anywhere within the array and because the neutral cross-scattering is 10 to 20%, a correction factor must be applied for the relative losses of neutrons out of the side of the array; this loss in each case was computed from the measured neutral cross-scattering distribution. The relative correction was between 2 and 5% with an error of 1%.

The distribution of events in the hydrogen target and consequently the absorption of neutrons leaving the target were different for the calibration and photoproduction experiments. This difference in distributions was due to the different beam profiles, the geometric selection of events by the proton telescope, and (usually) use of only the downstream half of the target in the main experiment whereas the target was full during calibration. The interaction of neutrons was included in Monte Carlo calculations describing both experiments, and allowed a relative correction to be made (less than 1%).

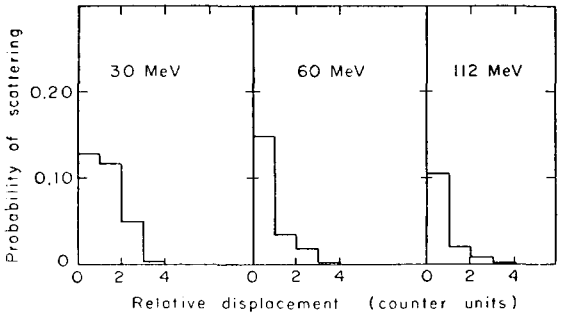

Fig. 10. Neutral cross scattering probability distributions.

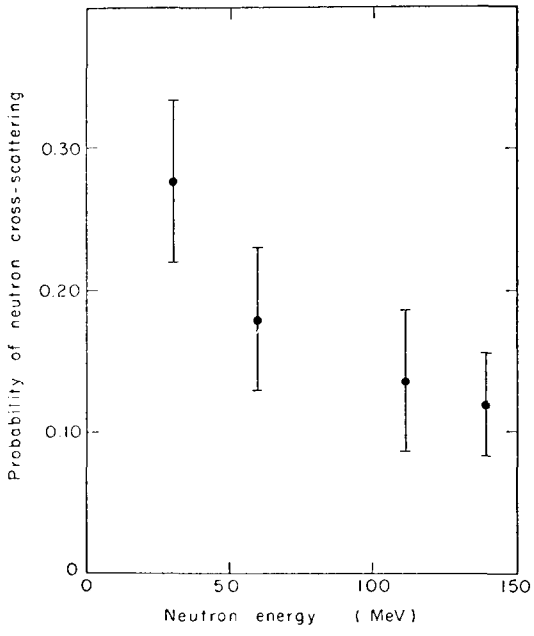

Fig. 11. Total probability of neutral cross scattering vs energy, i.e., ratio of counts in secondary counters to counts in primary counter.

8. Summary

The method of construction and operation of the neutron counters has proved reliable and repeatable in terms of counter efficiency and time resolution. The calibration experiment has shown that the neutron-counter array fulfilled the requirements of the experiment for which it was designed. Also, the successful application of the above-mentioned corrections demonstrated the possibility of using the same counters in other configurations.

We are grateful to Mr. R. Belisle, Mr. C. Brazell, and Mr. R. Roberts for valuable technical assistance and to Mr. N. Gunther for much of the computer programming effort. We also wish to acknowledge the support of Mr. J. Vale and the crews of the 184-inch

cyclotron, and the LRL and UCLA computing facilities.

References

[1]) C. E. Wiegand, T. Elioff, W. B. Johnson, L. B. Auerbach, J. Lach and T. Ypsilantis, Rev. Sci. Instr. **33** (1962) 526.

[2]) P. H. Bowen, G. C. Cox, G. B. Huxtable, A. Langsford, J. P. Scanlon, G. H. Stafford and J. J. Thresher, Nucl. Instr. and Meth. **17** (1962) 117.

[3]) J. B. Czirr and D. R. Nygren, Nucl. Instr. and Meth. **31** (1964) 226.

[4]) D. E. Crabb, J. G. McEwen, E. G. Auld and A. Langsford, Nucl. Instr. and Meth. **48** (1967) 87.

[5]) F. P. Brady, J. A. Jungermann, J. C. Young, J. L. Ronero and P. J. Symonds, Nucl. Instr. and Meth. **58** (1968) 57.

[6]) D. Bollini et al., Nuovo Cimento **61** A (1969) 125.

[7]) C. E. Wiegand et al., loc. cit.; F. P. Brady et al., loc. cit.

[8]) Obtained from Nuclear Enterprises, Ltd., Winnepeg, Manitoba, Canada.

[9]) Obtained from EG&G Inc., 35 Congress St., Salem, Mass., U.S.A.

[10]) Calculation made with computer program by R. J. Kurz, Lawrence Radiation Laboratory Report UCRL-11339 (March 1964).